Conceptual Design Report: Radial RF Injectors for Improved Waste Stream Processing

J.W. Lewellen, Los Alamos National Laboratory, PI
J.R. Harris, Air Force Research Laboratory, Co-PI

Work performed under the Department of Energy, Office of Science Accelerator Stewardship Program
DOE National Laboratory Program Announcement LAB 17-1779

01 October 2018

LA-UR-18-30012

(this page intentionally left blank)

Technical Team

Los Alamos National Laboratory (LANL)

J.W. Lewellen, LANL Lead
F.L. Krawczyk

Air Force Research Laboratory (AFRL/RDH)

J.R. Harris, AFRL Lead
J.M. Connelly

AFRL Contractors

W.E. Sommars, Leidos, AFRL Contractor Lead
R.B. Miller, EBM, LLC
N.T. Myers, Verus Research

Table of Contents

Table of Figures vi
Introduction 1
Physics Design and Simulations 3
Fundamental Concepts 3
Cavity design 3
Electron source 3
Simulations 4
Cavity 4
Electron source and initial transport 5
Beam dynamics 6
Cold-Test Model Measurements 8
Cavity mode spectra 8
Cavity Q 9
Beadpull measurement 10
Key Engineering Calculations 11
System Architecture, Diagnostics, and Controls 11
Structure Design Considerations 17
RF Frequency Selection 17
RF Power Consumption 18
RF power couplers 19
RF Power and Phase Stability 19
Beam Exit Window Options [] 19
Radiation Shielding and Beam Loss 21
Operational Estimates 22
Scheduled Maintenance Intervals 22
Achievable Uptime 22
RF systems 22
Cryogenics 23
Beam Generation 23
Controls and Power Supplies 24
Other Sources of Downtime 24
Staffing Requirements for Operations and Maintenance 24
Cost Estimates 25
Capital Costs 25
Operating Costs 25

Manpower (Operations Staff) 25
Service and Repair 25
Electrical 25
References 27

Table of Figures

Figure 1: Radial RF gun initial concept. 1
Figure 2: (a) electron range in water as a function of energy, over the range of Type 1 and 2 accelerators; (b) target geometry for a linear beam source; (c) target geometry for a radial beam source. d_{pen} is the beam penetration depth; r_{inner} is the radius of the waste stream pipe. 2
Figure 3: Perspective view of the 2-cavity radial RF gun. Different colors indicate different cavities. 4
Figure 4: Cross-sectional view; all dimensions are in cm. 5
Figure 5: Radial field as a function of position along the beam tube for inner (black) and outer (red) cavities, normalized to the peak field along the beam tube axis. 5
Figure 6: Cross-section of the conceptual electron gun. The emission area is in red. 6
Figure 7: (a) Beam energy and (b) RMS (black) and FWFM (red) energy spread as functions of radial position. 7
Figure 8: Beam envelope in "horizontal" (top) and "vertical" (bottom) local planes as a function of radial position. "Scalloping" is from histogrammed timestep output. 7
Figure 9: 3D printed cavity model half with scale (left) and installed in bead-pull apparatus (right) 8
Figure 10: outer (left, top and bottom) and inner (right, top and bottom) cavity mode spectra. 9
Figure 11: Beadpull measurement, compared to calculated fields from CST Microwave Studio. 10
Figure 12: Multiple radial electron guns for redundancy 11
Figure 13: Some possible configurations for treatment volume within radial gun. 12
Figure 14: Nonuniform dose profiles resulting from a few discrete beams in a flue gas stream, as calculated by MCNP6. 13
Figure **15**: Odd number of beamlets allow integrated diagnostics. 13
Figure **16**: Multiplate diagnostic. (Top Left) Simulated dose deposition for a 24 MeV electron beam. (Top Right) Simulated dose deposition for a 48 MeV electron beam. (Bottom Left) Experimental prototype. (Bottom Right) Experimental prototype deployed on the 25 MeV electron linac at the Idaho Accelerator Center. 14
Figure 17: Overview of emergency shutdown and restart procedures. (a) System configuration, showing bypass loop. (b) Normal operation. Green arrows indicate treated waste while red arrows indicate untreated waste. The bypass loop is valved off and the bypass loop pump is off. (c) A fault condition shuts down the RF guns, and untreated waste begins flowing past them. (d) This triggers closure of the fast-acting valve, which closes shortly after the fault is detected but prior to untreated waste leaving the system. (e) Input and output valves are closed to prevent any new material from entering the system during restart. (f) The bypass loop is activated. (g) The RF guns are reactivated. As waste material circulates through the bypass loop, more of the material in the system is treated. (h) Ultimately the entire system contains only treated material. (i) The bypass loop is disabled, the input and output valves are opened, and normal operation is resumed. 16
Figure 18: equatorial (left) and polar (right) view of X-ray dose maps. 21

Introduction

In June 2017, the US Department of Energy Accelerator Stewardship Program [1] released its "FY2017 Research Opportunities in Accelerator Stewardship" [2], including a call for design studies of four types of high-power electron accelerators for energy and environmental applications. Table 1 lists the target performance for the "Type 1" and "Type 2" accelerators in this call.

Table 1: Desired parameters for type 1 & 2 accelerators.

	Type 1 Demo/Small Scale	**Type 2 Medium Scale Low Energy**
Electron Beam Energy	0.5 – 1.5 MeV	1 – 2 MeV
Electron Beam Power (CW)	> 0.5 MW	> 1 MW
Wallplug Efficiency	> 50%	> 50%
Target Capital Cost[1]	< $10/W	< $10/W
Target Operating Cost[2]	< 1.0 M$/yr	< 1.5 M$/yr

[1] Including all supporting systems, e.g. power, cooling.
[2] Including all labor, supplies, repair, electricity, etc.

In response to this call, we proposed to study the application of a novel radial RF electron gun [3] to this mission. In this role, the radial RF beam source (hereafter referred to as a "radial gun") is intended to improve our ability to implement electron beam irradiation treatment of flue gasses, wastewater, or other materials amenable to being directed as a flow past an irradiation source.

Conventional electron beam sources typically take on the same basic form as a linear accelerator, generating a "pencil" beam along a single well-defined axis. While this is ideal from the standpoint of injecting a beam into a higher-energy accelerator, it poses several issues regarding the use of the beam for waste stream processing.

In contrast, a "radial" RF-driven electron beam source uses one or more annular RF cavities delivering a beam towards the axis of the annulus; Figure 1 shows an early concept for such a device.

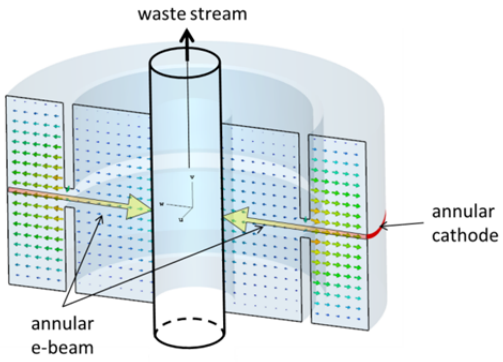

Figure 1: Radial RF gun initial concept.

We believe such a design has significant advantages for waste-stream processing, which are encapsulated in Figure 2. In short, a linear beam source requires (1) overpenetration of the waste stream to deliver dose to all portions of the stream, wasting beam power and increasing radiation protection issues downstream of the waste stream; (2) energy loss and beam scattering along the beam path will lead to dose nonuniformity in the waste stream, further increasing the required peak dose; and (3) waste stream cross-sectional area scales linearly with the beam energy.

A radial beam source, in contrast, (1) can be designed such that all of the waste stream can receive dose while completely absorbing the beam within the stream, eliminating the need to fully overpenetrate the treatment volume and the resulting power and radiation protection issues; (2) has the potential for greater dose uniformity, further reducing the required peak dose; (3) the waste-stream area scales with the square of the beam energy; (4) a radial system is somewhat self-shielding, since radiation is primarily directed inward towards the center of the system, and must therefore pass through the treatment volume, and through the RF cavity walls on the other side before exiting the system; and (5) the added complexity of the raster-scanning mechanism is eliminated.

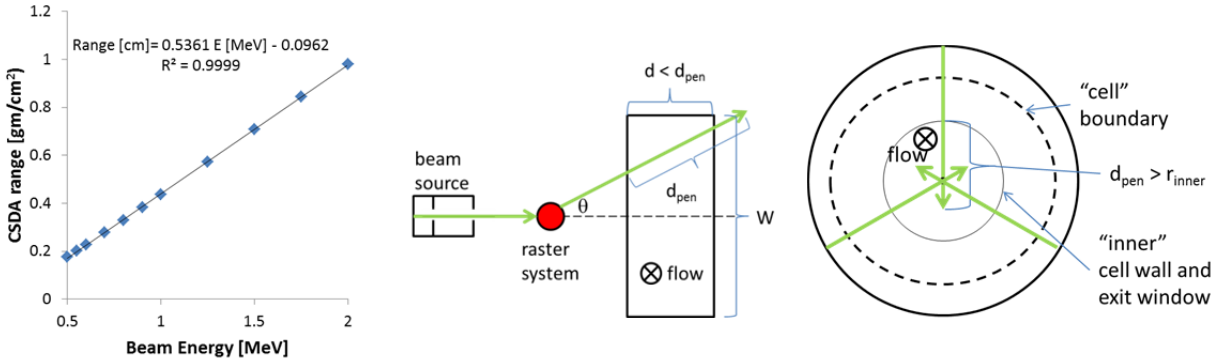

(a) (b) (c)

Figure 2: (a) electron range in water as a function of energy, over the range of Type 1 and 2 accelerators; (b) target geometry for a linear beam source; (c) target geometry for a radial beam source. d_{pen} is the beam penetration depth; r_{inner} is the radius of the waste stream pipe.

This conceptual design report represents the results from a one-year study of this concept, focusing on the basic feasibility via electron beam dynamics simulations and dose delivery. Estimates are also provided for operational considerations such as capital and operating costs, required diagnostics, etc.

Physics Design and Simulations

This section describes our initial exploration of the radial RF gun in a pollution control application, guided by the desired parameters from Table 1. For an actual system, this design may need to be modified to incorporate additional relevant engineering concerns, some of which are addressed later in this report. This section incorporates an expanded version of a paper presented at the IPAC 2017 conference [4].

Fundamental Concepts

The preliminary radial RF gun design is based around the use of coaxial $\lambda/2$ resonator cavities. We note that our design bears superficial resemblance to the Rhodotron [5], which also makes use of a coaxial $\lambda/2$ resonator. However, Rhodotrons are typically intended to operate in the 3 – 10 MeV range, with beam powers to several hundred kW, so are higher-voltage, lower-current machines compared to our design. Also, the Rhodotron directs the beam through multiple transits of the coaxial resonator to obtain the desired beam energy, and produces a "pencil" beam as its output. Since our design is intended to have a target along the axis of the resonator, we cannot make use of this elegant approach.

We selected an operating frequency of 350 MHz, as MW-class CW klystrons at this frequency are commercially available and in service in storage rings. Further, in this frequency range, superconducting structures can be efficiently operated at 4 K, and normal-conducting cavities are also potentially feasible due to the relatively low wall losses.

Cavity design

The basic form of the cavity is a half-wavelength coaxial resonator with length L_{cav}, and inner (outer) radii $r_{i(o)}$. The mode of interest has electric fields $E_z = E_\phi = 0$, and

$$E_r(r,z,t) = \frac{E_n}{r} cos\left(\frac{\pi}{L_{cav}} z\right) cos(2\pi f_o t + \varphi) \quad (1)$$

for $|z| < L_{cav} / 2$ and $r_i \leq r \leq r_o$, E_n is the magnitude of the field at unit radius, $f_o = {}^{c}/_{2L_{cav}}$ is the resonant frequency, and φ is a constant phase offset.

The notional cavity shown in Figure 1 is a 2-cell coupled-cavity coaxial resonator, the radial RF gun equivalent of a 1½-cell photoinjector cavity. In practice, while we found it possible to generate such a coupled cavity design, as in the 1½-cell photoinjector, the field balance between the cells is quite sensitive to the details of the geometry. Therefore, we decided to focus upon the use of either single cavities, or multiple cavities that are independently powered and phased. In practice, the ability to independently phase the cavities also allows for greater flexibility of operation, for instance, final beam energy with good energy spread.

Electron source

The conceptual design shown in Figure 1 shows an annular cathode. While ideal in concept, in practice it does not appear practical. Rather, for our initial cavity design we considered using N cathodes spaced at 360/N degrees around the equator of the cavity as the beam source. For $N \geq 6$ we should have a reasonable approximation of an annular beam by the time the beams reach the target at the axis of the cavity.

As the eventual goal is the design of an industrial beam source, we wish to use thermionic cathodes rather than photocathodes. Given that the RF cavities may be superconducting, however, we require both thermal isolation, and short emission windows (relative to the RF period) to minimize "tails" and beam loss inside the cavity. (Generally, we note that these characteristics represent good "beam hygiene" regardless of whether the cavity is normal- or superconducting.) To that end we have also developed a conceptual design for a relatively low-voltage (~25 kV) DC gun based around a gridded cathode. This design, in simulation, works well for an initial design concept with N=6; as N is increased, the per-gun performance requirements are eased.

If the total beam current is to be on the order of 1 A, then for N~6 each cathode must supply on the order of 0.1 – 0.2 A. At 25 kV, this corresponds to beam power on the order of 5 kW per gun, well within the range of commercial power supplies. If all of the guns are ganged together, then at 25 kV the gun HV power supply would be required to source on the order of 25 kW, also feasible. The specific choice will likely be deferred to operational concerns, e.g. desired behavior should one gun experience an arc.

Per-cathode beam currents of 0.1 – 0.2 A correspond to bunch charges of 0.3 – 0.6 nC. We wish to have bunches shorter than about 40° relative to the cavity RF period to help control energy spread and differential focusing, corresponding, at 350 MHz, to 300 ps, or peak beam currents of around 1-2 A.

Operating at this voltage allows us to drift the beam from the gun through a reasonable distance to the cavity entrance, allowing for thermal isolation, and access to the cathode from outside of the cryogenic enclosure for easier maintenance.

Simulations

Cavity

We chose elliptical toroids for our basic cavity design, similar in cross-section to linear superconducting cavities. Our initial design has both an inner and an outer toroid, each with six beam tubes. Figure 3 shows a 3-d perspective view; Figure 4 shows the fields in cross-sectional slices, and Figure 5 shows the normalized radial field, $E_r(r)$, along one of the beam tubes. CST Microwave Studio [6] was used to perform the cavity modeling.

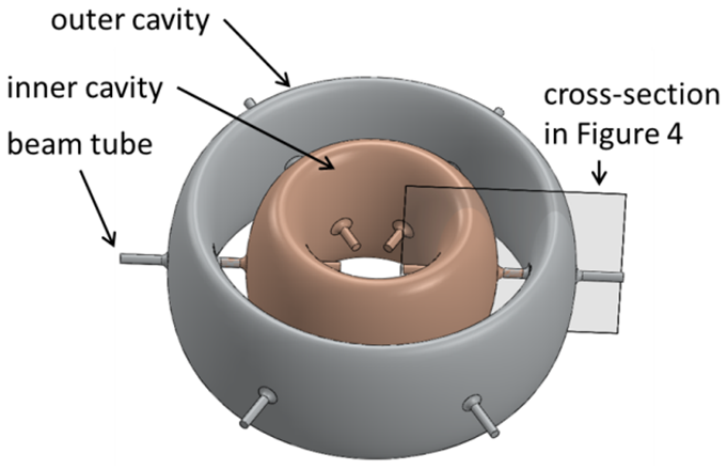

Figure 3: Perspective view of the 2-cavity radial RF gun. Different colors indicate different cavities.

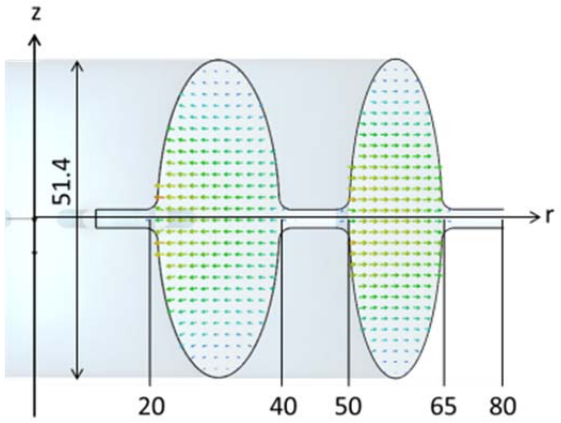

Figure 4: Cross-sectional view; all dimensions are in cm.

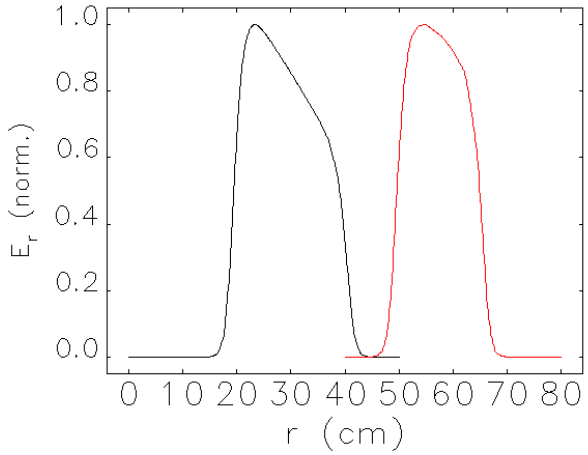

Figure 5: Radial field as a function of position along the beam tube for inner (black) and outer (red) cavities, normalized to the peak field along the beam tube axis.

The cavities' lengths (z-extent in Figure 4) were individually optimized to have their fundamental modes resonant at 350 MHz. The cavity radial separation is shown as 10 cm; the separation could be increased to accommodate a small inter-cavity solenoid, or to increase cavity-to-cavity RF isolation if necessary. The radial dependence of E_r is clearly visible in Figure 5.

Finally, while the cavity shown in Figure 3 has six beam tubes, the cavity could readily support up to at least 12-15 ports; doing so trades off a lower per-cathode beam current, versus greater heat leakage from outside the cryostat for a superconducting structure. The dependence of resonant frequency upon the number of beam tubes is small, on the order of 10 kHz increase per beam tube added; in any event, a design intended for fabrication would be frequency tuned taking into account the number of beam tubes. Engineering concerns, to be discussed below, suggest the use of an odd number of beam tubes.

Electron source and initial transport

The cathode emission parameters are described above. Our initial source design is based around the use of a Pierce-like 25-kV DC gun, plus a small solenoid to aid transport prior to beam injection into the outer cavity.

The gun, simulated using Poisson [7], has a cathode/anode cone angle of 50° (measured from the axis), a 1-cm accelerating gap, and an 0.56-cm radius cathode located at r = 80 cm. The solenoid is 2 cm long, and centered at r = 72.5 cm. A conceptual cross-section is shown in Figure 6.

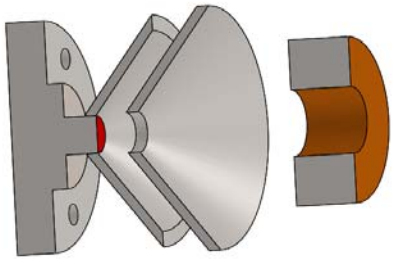

Figure 6: Cross-section of the conceptual electron gun. The emission area is in red.

For comparison, commercial products such as the Model HWEG-1228 e-gun from HeatWave Labs [8] exhibit comparable performance in terms of duty factor, voltage, and perveance. We assume the use of a gridded cathode, so as to be able to gate emission.*

Beam dynamics

The General Particle Tracer (GPT) code [9] was used to perform beam dynamics modeling from the cathode grid at r=80 to r=0, using 300-pC bunches and 300-ps emission times, and a 25-kV DC gun voltage. This corresponds to a per-gun peak (average) current of 1 A (0.105 A). The gun solenoid had a peak field of 225 gauss; the on-axis field at r=65 cm (boundary of the outer cavity) was approximately 10 gauss. The peak on-axis fields in the outer and inner cavities were 4.5 MV/m and 4.8 MV/m, respectively, and were phased for maximum beam energy gain. The results shown were generated by tracking 50k particles, using GPT's 3-d mesh space charge routine and the fields calculated with CST and Poisson for the cavities and DC gun, respectively. GPT's `bzsolenoid` element was used to approximate the gun solenoid. (Simulations with 0.6-nC bunches also show acceptable transport.)

In Figure 7 and Figure 8 below, the beam is propagating from left to right, and properties are plotted vs. the radial coordinate axis in Figure 4.

Figure 7 shows the beam energy and fractional energy spread as a function of radial position.

The beam envelope is plotted in Figure 8 using a local Cartesian coordinate system aligned with one beam tube. In both the horizontal (perpendicular to z-r plane in Figure 4) and vertical (parallel to the z axis in Figure 4) local directions the beam core is well confined; the full beam radius does not exceed the nominal beam pipe radius of 1.5 cm. The inner cavity ends at r=20 cm, so, if required, an additional solenoid could be placed before the exit window to spread the beam for a more uniform dose delivery.

This 2-cell design can easily meet the requirements of either a Type 1 or Type 2 source from Table 1; it appears likely a 1-cell design could also meet the Type 1 requirements.

* We have developed a concept for an RF harmonic-based gating scheme that, in principle, can extend to very short pulse generation; however, for this application, more conventional approaches (single RF frequency + DC offset) should suffice.)

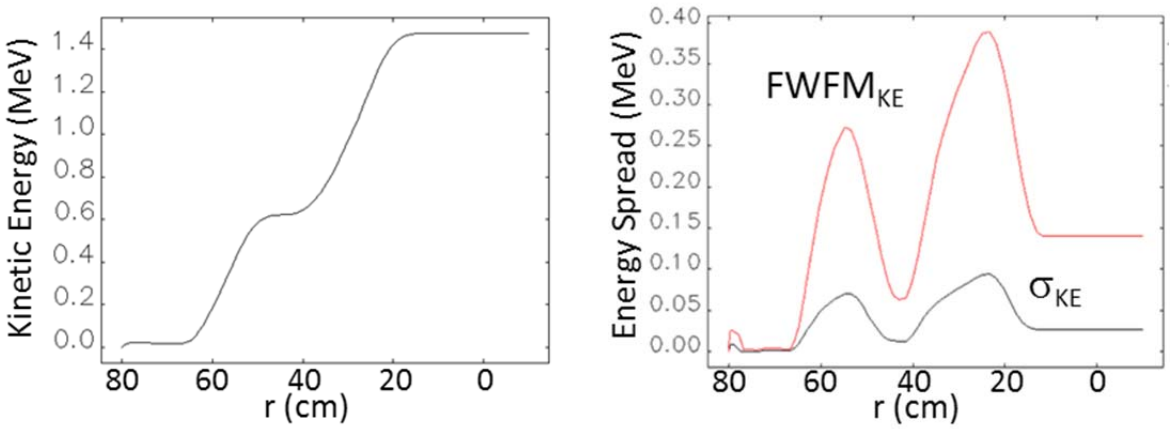

(a) (b)

Figure 7: (a) Beam energy and (b) RMS (black) and FWFM (red) energy spread as functions of radial position.

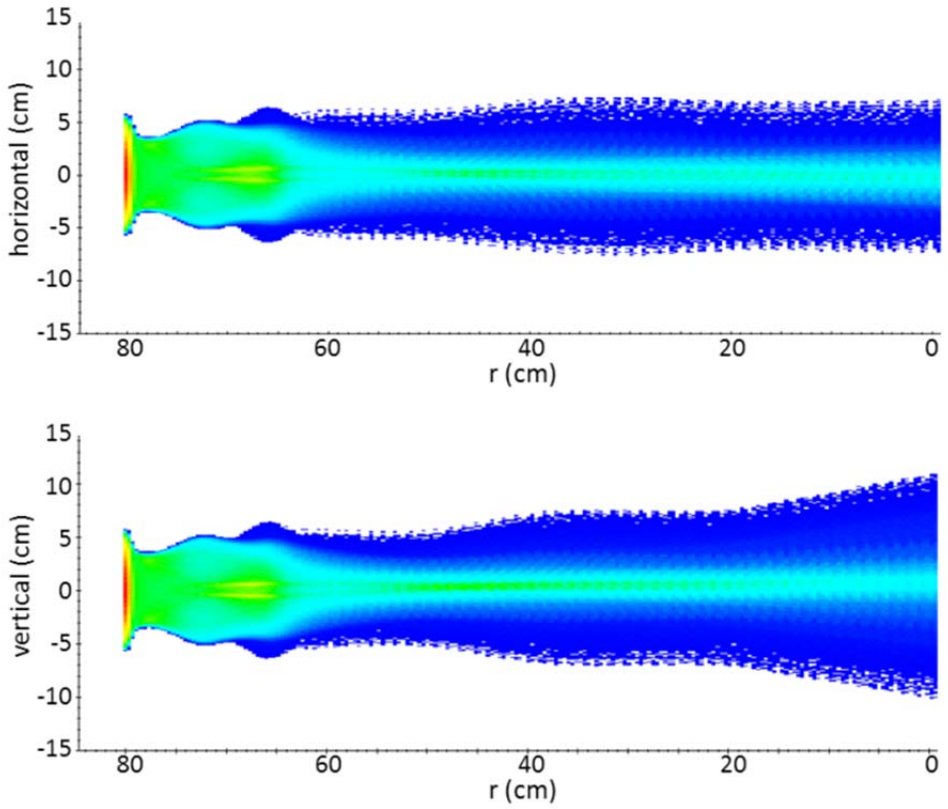

Figure 8: Beam envelope in "horizontal" (top) and "vertical" (bottom) local planes as a function of radial position. "Scalloping" is from histogrammed timestep output.

Cold-Test Model Measurements

Modern 3D RF modeling codes such as CST are generally very accurate; however, the radial RF gun is a fairly unusual geometry, and we fabricated several approximate 1/10-scale cavity models to, first, verify the geometric design and, second, to perform cold-test measurements.

The radial RF gun geometry naturally lends itself to a "clamshell" fabrication method, reminiscent of that used in [10] wherein pillbox cavities are split longitudinally rather than equatorially. In both cases, there is nominally no RF current flow across the joint; this contrasts with the "cup" method traditionally used for pillbox cavity structures, wherein cylindrically symmetric sections are brazed together, and surface currents flow through the brazed joints. This results in the configuration in Figure 9, which shows a 3D printed plastic cavity half with scale, and being used to pre-align a beadpull apparatus. This plastic prototype served to check the mechanical design, and is planned for a future test in which it will be coated with conductive paint and tested in comparison to the primary, aluminum cold test cavity.

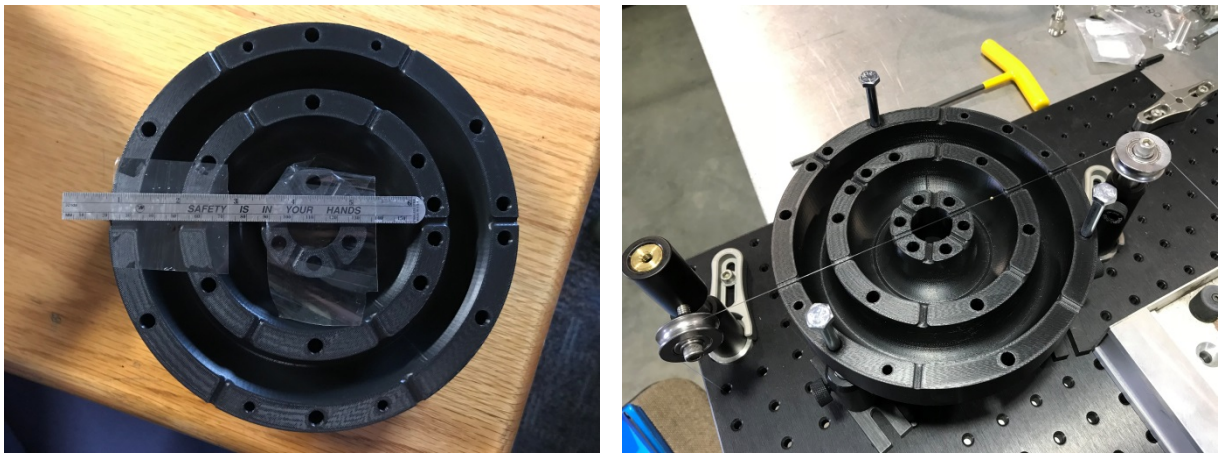

Figure 9: 3D printed cavity model half with scale (left) and installed in bead-pull apparatus (right).

The aluminum cold test prototype was built and successfully tested. Measurements were conducted with an "uncalibrated" network analyzer, (e.g. cal kit not used) since we were significantly varying the range of frequencies, coupling, etc. throughout the measurements. The measurements of interest, generally speaking, do not require absolute phase or power measurements, and therefore calibration, while useful, is strictly speaking not necessary.

The exact cavity scaling factor was chosen to result in a beam tube diameter equal to that of RG402 rigid coax [11], 3.58 mm, so as to allow us to use stripped RG402 lines as field probes and power couplers by simply clamping them between the structure halves. The cavity halves were clamped and separated several times in order to move field probes, etc., with generally excellent repeatability. We also note that the cold-test model validates one of the RF power coupler concepts for the radial RF gun: an antenna-type coupler inserted into either an existing beamtube, or a specific coupler port at the cavity midplane and azimuthally between two beamtubes.

Cavity mode spectra

Figure 10 shows the mode spectra of the outer and inner cavities, measured via both S11 (reflected power) and S21 (transmitted power).

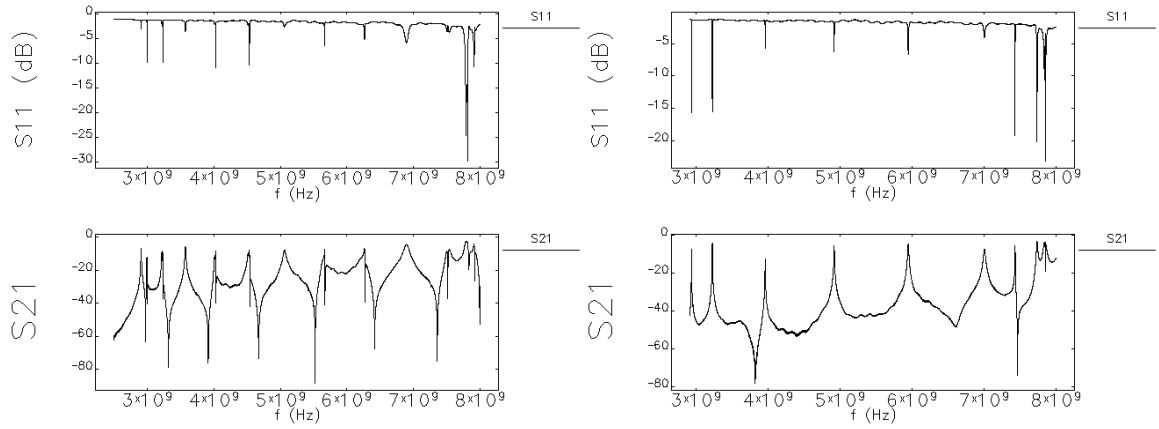

Figure 10: outer (left, top and bottom) and inner (right, top and bottom) cavity mode spectra.

We expect a field probe extended through a beam port, would in general only be able to pick up modes with strong radial fields in the midplane of the cavity. Running CST Microwave Studio in "eigenmode" mode will find these modes as well as others, e.g. with no radial field components. Table 2 lists the frequencies of identified modes (for the scaled cavity model) with strong radial fields, and compares them to the modes found in the cold-test cavity spectra. CST was asked to calculate the frequencies of the 20 lowest modes; modes without strong radial fields are not included in the table.

Generally speaking, the agreement in frequency between measured and predicted mode spectra are very good to excellent, for both inner and outer cavities.

The first mode frequency measurement in the table is taken from our beadpull runs. As machined, the cavities are 0.5 MHz apart in frequency, a relative difference of 0.016%.

Cavity Q

For an ideal cavity fabricated from aluminum (using conductivity of 3.77 x 10^7 S/m, courtesy of Wikipedia), CST predicts a Q_0 of 6500 for the outer cavity, and 8000 for the inner cavity.

We estimate a measured Q_0 of 6000 for the outer cavity, and 6800 for the inner cavity, depending on the specifics of how the coupling was set up, S11 vs S21 measurement, etc. This is in reasonable agreement with the CST calculation, given the physical cavity's equatorial break. Time permitting, we will revisit this measurement using conductive paint to improve the cavity half connection; this degree of reduction, however, is reasonable and consistent with past experience of brazed vs. mechanically clamped cavities.

Table 2: A comparison of calculated and measured resonant frequencies. All values are in GHz.

Outer cavity		Inner cavity	
CST frequency	measured	CST frequency	measured
2.93	2.936746	2.934	2.936242
3.01 *	2.98	3.22 / 3.23 *	3.22
3.24 *	3.22 / 3.23	3.962 / 3.966 *	3.95
3.59 *	3.57	4.91 / 4.92*	4.91
4.04 *	4.03	5.95/5.96 *	5.94
4.54 *	4.53	7.016 / 7.017	6.99
5.09 / 5.10 *	5.06		
5.67 *	5.66		

* = degenerate modes (rotation about the z-axis)

Beadpull measurement

Figure 11 shows the measured field profile, based on $E_z(r) \propto \sqrt{|f_o - f(r)|}$, where f_o is the unperturbed frequency and f(r) is the frequency when the bead is at the radial position r. (Strictly, the absolute value bars shouldn't be necessary, since the frequency shift should always be to lower frequency. However, this is the formulation we used in Excel, as at small frequency shifts, random errors would occasionally give a negative quantity inside the root.)

The points are the measured data; the solid lines are the fields calculated by CST Microwave Studio, scaled to the same peak values as the measured data. The CST fields, as shown, reference their positions to the center of the structure at r=0.

The bead used was a clipped spherical "sinker," 2.8 mm in diameter by 2.3 mm long, with an approximately 1 mm aperture in the center for the line.

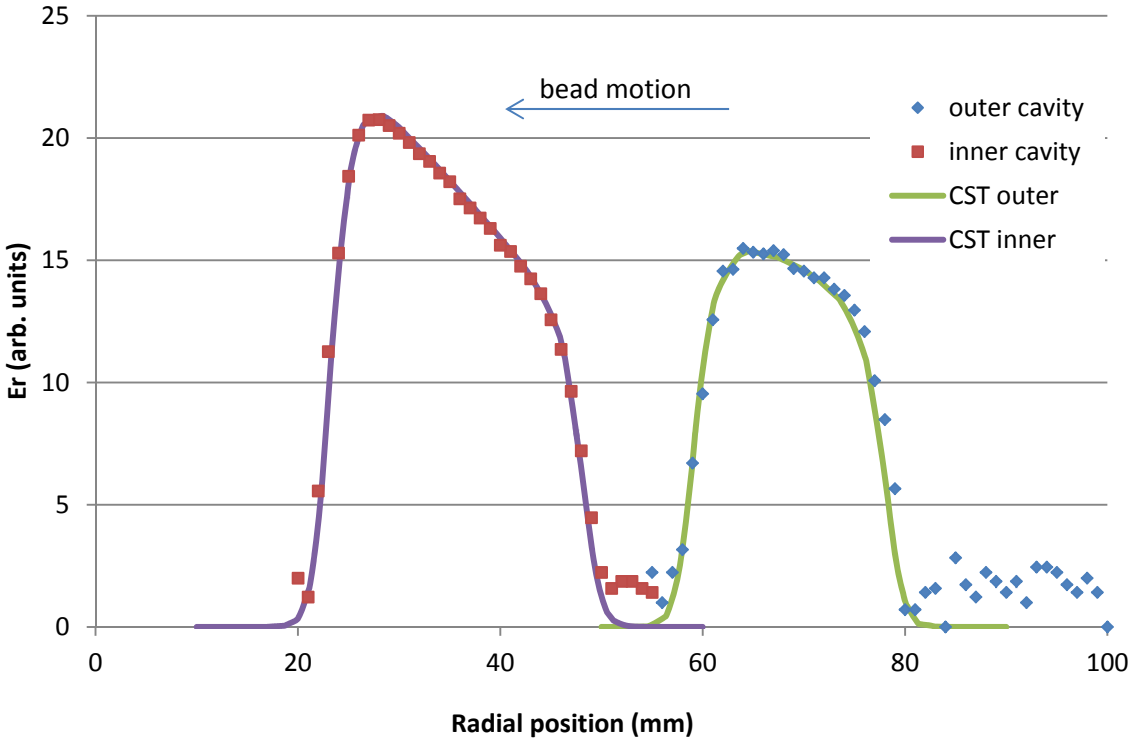

Figure 11: Beadpull measurement, compared to calculated fields from CST Microwave Studio.

Key Engineering Calculations

System Architecture, Diagnostics, and Controls

The radial RF gun concept as discussed here admits several system architecture options which may provide additional benefits in the pollution control role.

First, it is possible to use two or more radial guns, mounted coaxially along the direction of flow of the treatment volume. Such "stacked" guns would enable the total dose delivered to the treatment volume to be shared among multiple guns, thus greatly reducing power, cooling, beam current, and beam window stress requirements per stage. The guns could also be "clocked" such that beam ports are offset azimuthally from one gun to the next, allowing more thorough irradiation in the region near the beam windows.

If each gun were additionally operating significantly below its maximum capabilities, the loss of one gun could be compensated for by increasing power and therefore dose delivered by the remainder of the guns to ensure that the total dose absorbed by the treatment volume during its passage through the system would remain constant. An economic tradeoff study is necessary to identify the optimal number and configuration of guns in such a "stacked" configuration, which is beyond the scope of the present study.

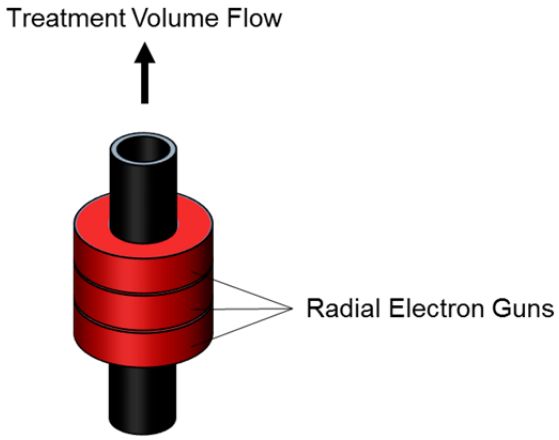

Figure 12: Multiple radial electron guns for redundancy

Note that the pipe containing the waste stream does not have to be a simple cylinder with an outer diameter equal to the gun inner diameter, although that is certainly one option. A simple cylinder of reduced diameter could also be used, and may be preferred for lower energy operation, which implies a shallower penetration depth of the beam in the treatment volume. The added distance between the cavity and the treatment volume could allow beam spread, either due to space charge, deliberate overfocusing of the beam (ie, pinching the beam to a tight waist so it will expand rapidly downstream of the waist), or through insertion of scattering materials. The treatment volume could also take the form of a thin shell, which again has advantages for low energy operation, but may increase the likelihood of dose nonuniformity. Figure 13 illustrates these options. Vanes may also be introduced into the pipe to force some degree of laminar flow, which is particularly important if "clocking" of subsequent cavities is used to offset azimuthal dose nonuniformities. Allowing the treatment volume configuration to differ from the cavity dimensions is particularly important as it allows, to some extent, increased design flexibility in both the RF gun and waste handling subsystems.

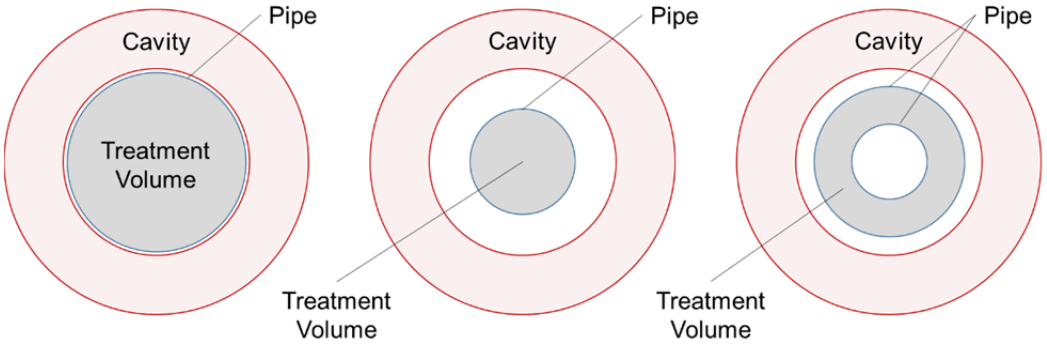

Figure 13: Some possible configurations for treatment volume within radial gun.

The use of multiple discrete, rather than a single circumferentially-continuous, beam sources also provides advantages, particularly when an odd number of cathodes are used, for several reasons. First, the loss of a single beam source does not require the system to shut down. If each beam source is operating significantly below its maximum current, loss of a single beam source could be offset by increasing the dose delivered by the remaining beam sources in a single gun, or by increasing the dose delivered by the other guns in a multiple-gun system. Care would be needed in designing such a system, since loss of a single beam source may increase dose nonuniformity. This may drive the design towards the use of a higher number of beam sources.

Use of an odd number of beam sources may increase system resiliency by enabling operation when the target volume density or type has changed (for example, due to changes in pressure when a gaseous target volume is used, or due to running a liquid-based system that has not yet been charged with liquid). In either condition, some or all of the beam coming from one particular cathode will travel across the system interior, but due to the odd number of cathodes, very little of it would be incident on the beam window associated with another cathode. This not only avoids delivering excessive energy to a beam window, possibly leading to its failure, but also prevents the counterpropagating beam from propagating upstream, in which case it could gain energy from the RF fields in the cavity depending on its arrival phase, and deliver energy to the opposing cathode, damaging it.

Note that one disadvantage of the discrete beam source configuration is the likelihood of increased dose nonuniformity, as illustrated in Figure 14. In a multiple-gun installation, this can be offset by "clocking," or azimuthal rotation, of subsequent guns, as well as incorporation of beam “pinches” and scatterers. Note that this assumes laminar flow of the treatment volume.

Additionally, use of an odd number of beam sources introduces the possibility of placing beam / dose diagnostics at locations opposite each beamlet, illustrated in Figure 15. While the signals produced from such diagnostics would not provide direct indications of dose delivered to the treatment volume, they could be calibrated to provide an indication of this dose. They would also provide real-time feedback on each beam source and cavity. As the signal detected by these diagnostics would depend on beam energy and treatment material density, it could provide online warning indicators of changes in beam energy or target volume density which might indicate or lead to a fault condition. Even if the primary beam is not able to pass across the entire treatment volume diameter, as envisioned here, the resulting secondary radiation shower might be able to, and might be detectable by the diagnostic. Additionally, with no treatment material present (ie, an uncharged liquid-based system), these diagnostics could be used to tune up the system.

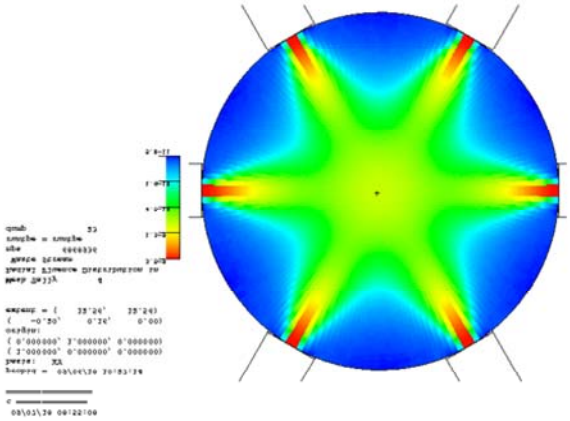

Figure 14: Nonuniform dose profiles resulting from a few discrete beams in a flue gas stream, as calculated by MCNP6.

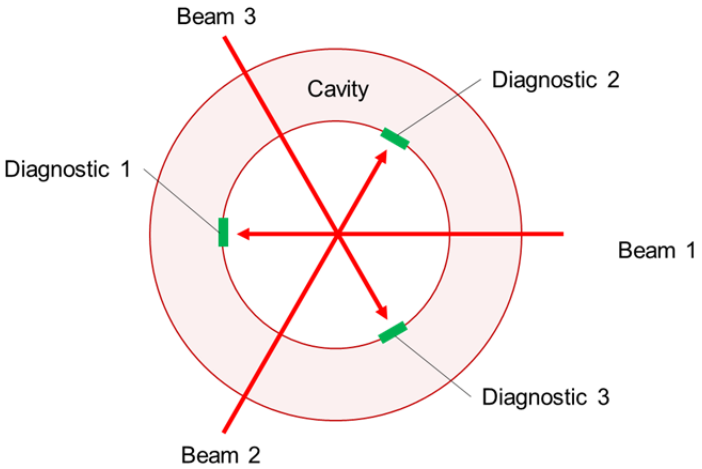

Figure 15: Odd number of beamlets allow integrated diagnostics.

One potential beam diagnostic that could be used in this role is a multiplate energy diagnostic. Shown below are simulations and a prototype of such a device, developed by Raytheon for AFRL under a separate contract [12,13,14]. This device uses a stack of thin aluminum plates to slow and stop an incident beam. As the beam propagates into the stack, it deposits charge onto the plates, with the charge deposition profile indicating the mean beam energy. Thus, this device could not only indicate the current reaching it (when operating as a Faraday cup) but also its mean energy, providing as a feedback signal for tuning up the gun, or flagging a fault condition in it. As a current-integrating diagnostic, it is capable of measuring and diagnosing very low currents, as demonstrated with the dark current on a 25 MeV S-band linac at the Idaho Accelerator Center. Note that the dose deposition in the plate stack in the absence of a treatment volume should also map onto the dose deposition across the target volume, with proper scaling, for the case of a monoenergetic beam. While the multiplate system as tested at Idaho has been optimized for higher-energy beams, scaling the design to lower beam energies appears to be feasible.

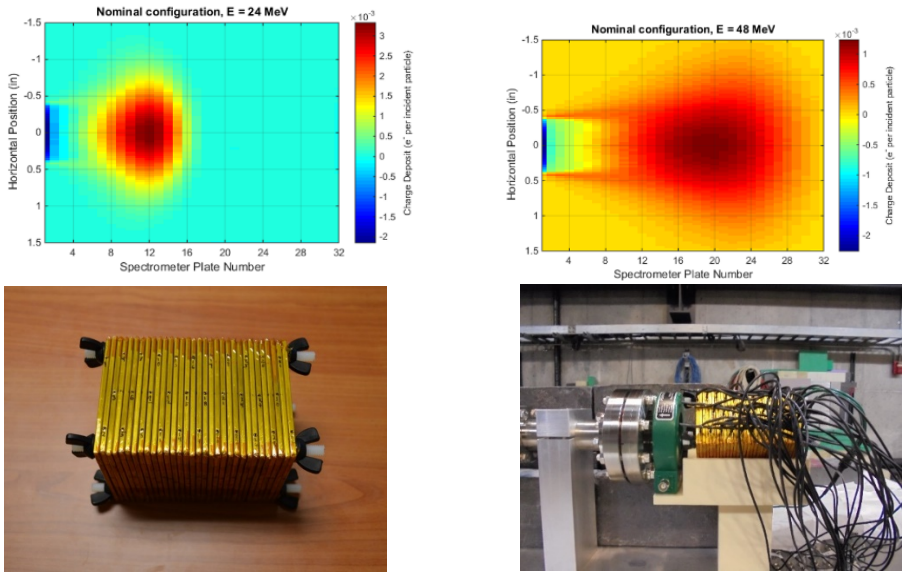

Figure 16: Multiplate diagnostic. (Top Left) Simulated dose deposition for a 24 MeV electron beam. (Top Right) Simulated dose deposition for a 48 MeV electron beam. (Bottom Left) Experimental prototype. (Bottom Right) Experimental prototype deployed on the 25 MeV electron linac at the Idaho Accelerator Center.

It would be desirable to automate system operation as much as possible, and for this the use of diagnostics and interlocks would be key. The system parameters that could be monitored for this include: (1) emitted current per beam source; (2) beam source voltage; (3) beam transport solenoid current, voltage, temperature, and cooling flow (if incorporated into the design); (4) RF cavity forward and reflected power; (5) transmitted current and mean energy from multiplate diagnostics as discussed above; (6) treatment volume flow rate; (7) residual radioactivity in the treatment volume downstream of the RF guns†; (7) radiation area monitors in the treatment facility; and (8) cavity cryogenic or cooling system status. These would be in addition to the standard personnel protection interlocks familiar to all accelerator operators. The details of these would depend on the actual system design, as well as regulatory requirements for the facility.

Abnormal indications from these diagnostics would trigger three general types of response, with those responses occurring automatically and indicated to the operators. The first category would be abnormal conditions not requiring immediate responses, for which warnings to the operators would be sufficient.

The second category would be conditions that could be corrected for by the system automatically, for example increasing power to the remaining cavities in the event of loss of one cavity.

The third category would be conditions which pose an immediate safety hazard, such as an excessive radiation level in the control room. This category would be highly unlikely to occur given the nature of the system considered here, but must be incorporated into its design. In such a situation, the treatment system would actually be taken offline and the waste stream flow must be halted. The waste handling system must be designed to accommodate this, for example by providing fast acting valves far enough downstream of the RF guns so that the mechanical system can halt the treatment volume flow before any untreated material propagates downstream to the system outflow. This means that for some distance downstream, the system will contain untreated waste, which traveled downstream between the time the electrical systems shut off the RF guns and the time the mechanical valves could stop the flow. This material must be captured and

† While we would not expect any residual radiation when operating below the neutron generation threshold, such monitoring could be part of a general policy of monitoring operation in an industrial setting where any release of radioactive material is unacceptable.

returned through the RF guns to be treated prior to release. Additionally, sufficient flow of treated material through this section must be used to ensure that any surface contamination of the pipe itself is dealt with. This argues for a bypass loop downstream of the fast-acting valve, which during restart can recirculate the untreated material which passed the RF guns until it is sufficiently treated, and the downstream pipes are sufficiently cleaned, to resume normal operation.

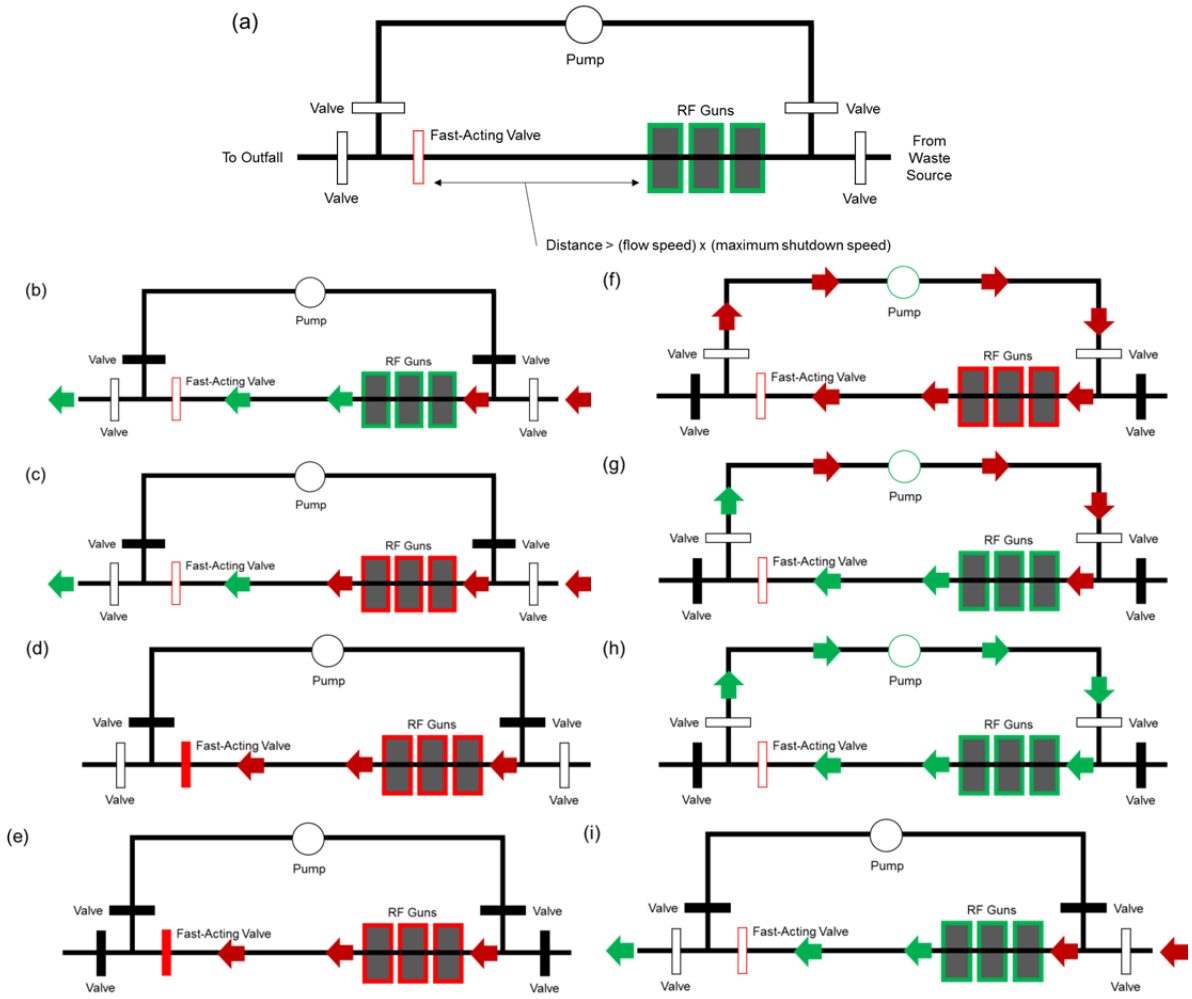

Figure 17: Overview of emergency shutdown and restart procedures. (a) System configuration, showing bypass loop. (b) Normal operation. Green arrows indicate treated waste while red arrows indicate untreated waste. The bypass loop is valved off and the bypass loop pump is off. (c) A fault condition shuts down the RF guns, and untreated waste begins flowing past them. (d) This triggers closure of the fast-acting valve, which closes shortly after the fault is detected but prior to untreated waste leaving the system. (e) Input and output valves are closed to prevent any new material from entering the system during restart. (f) The bypass loop is activated. (g) The RF guns are reactivated. As waste material circulates through the bypass loop, more of the material in the system is treated. (h) Ultimately the entire system contains only treated material. (i) The bypass loop is disabled, the input and output valves are opened, and normal operation is resumed.

Such a bypass system would likely be needed anyway for system startup and maintenance, for several reasons. During startup, the gun power may need to be ramped up slowly, meaning that the full, required treatment dose would not be delivered initially. Recirculating the flow would hold the overall treatment system in a standby mode until the full dose could be delivered, at which time the flow could be switched from the bypass loop to the outflow. Second, in some implementations the treatment volume flow will be needed to aid in cooling the beam windows. Insufficient flow during startup could lead to window failure and loss of one of more RF guns. In such a case, when running under automatic power control with multiple guns, a cascade failure could be triggered, where loss of a beam window on one gun due to insufficient window cooling would cause the remaining gun's powers to be increased, causing an additional window failure, and so on. Automatic power shifting should be disabled during startup for this reason. Third, the presence of a bypass loop would enable operation of the RF guns for testing and maintenance when the rest of the system

was not operational, enabling maintenance during periods when the waste-producing system is shut down, and at no risk of accidental outflow of untreated material.

By contrast, during normal operation a stable accelerator operating point would be selected, with the dose delivered to the waste stream fine-tuned by small changes in the waste stream flow rate. The user interface should be as simple as possible.

Structure Design Considerations

RF Frequency Selection

The initial design assumed an operating frequency of 350 MHz; 350-MHz, MW-class, CW RF klystrons have demonstrated good track records for operational lifetime and fault rates. In the range of 300 – 750 MHz, MW-class CW klystrons are still commercially available and are, at present, the most likely initial candidates for powering an industrial RF accelerator.

Historically, there have been multiple options for procuring klystrons of this type; several companies such as Thales, CPI and Toshiba produced high-power CW RF tubes (klystrons, IOTs, etc.), and large institutions such as SLAC and Fermilab have also fabricated their own tubes. In recent years, however, Thales appears to have cut back on their offerings of MW-class devices, and overall, worldwide availability of such tubes is decreasing [15]. In light of such developments, light sources such as the Advanced Photon Source at Argonne are considering switching to high-power solid-state RF sources [16].

During the initial beam dynamics simulations, we noted that not only the overall process, but also many of the beam source design "rules of thumb" translate fairly directly from conventional axially symmetric gun designs, to the radial RF gun. This suggests that radial RF guns operating at considerably higher frequencies are entirely feasible, allowing use of RF sources such as Toshiba's E37701, a 1.02-GHz, 1.2-MW tube; in turn, this should result in a considerably smaller physical device since the radial RF gun's length and diameter both scale inversely with frequency. There are two potential obstacles to this approach; both can be overcome, but one will require further R&D.

The easier obstacle to overcome is, simply, that operating a superconducting accelerator at frequencies above 500 – 700 MHz will generally dictate the use of a 2K (superfluid) helium system. In turn, this increases cryoplant operational complexity and the required input power. To obtain the same final beam energy, a higher-frequency accelerator generally requires a higher accelerating field because, all else equal, the wavelength and therefore accelerating gap is shorter. Therefore, expected RF losses will also be higher.

A related concern involves the maximum number of beam flight tubes; all else equal, the higher the frequency, the lower the number of beam flight tubes that can realistically be used. In turn, for a given beam power, this increases the per-tube beam current and potential for halo formation. Also, again all else equal, a smaller number of flight tubes will result in a less-uniform distribution of deposited power inside the volume to be irradiated. However, careful design of the beam transport and, if applicable, inserted scattering screens, can help mitigate these effects.

The other obstacle is the change in beam dynamics that will occur as one pushes towards higher frequency. For a given "phase length" of electron beam, at lower frequencies, the actual bunch length is longer; thus, at lower frequencies, it is simpler to obtain short (in phase terms) beams from thermionic gridded cathodes. Cathode-grid transit-time factors and voltage limits constrain how hard such cathodes can be driven, and in turn, how short of a beam pulse (in units of seconds) can be generated. Up to ~500 MHz, it appears we can generate the required bunch duration via relatively simple and proven methods with a gridded thermionic

cathode; at higher frequencies, however, either updated gating methods must be developed‡, or alternative cathode technologies such as photocathodes must be employed. Currently, the state-of-the-art does not suggest a photocathode-based approach would be viable in an industrial setting.

RF Power Consumption

There are two primary options for constructing the cavity: room-temperature copper, or superconducting niobium. To compare RF power consumption for these options, we used CST to calculate surface power dissipation for a copper version of the structures, and then used the ratio of the resistivities to estimate the power consumption for the superconducting version.

At frequencies above approximately 500 MHz, going to a 2K helium system is warranted by surface loss considerations; however, 2K refrigerators are considerably more complex, and require approximately double the input power per watt extracted from the cold mass, than 4K refrigerators.

Normal-conducting cavities

For the inner cavity, assuming the conductivity of copper (5.8 x 10^7 S/m), CST predicts losses of 75.7 kW for a peak "on-axis" field of approximately 1.85 MV/m. Scaling to the required 4.8 MV/m yields a power loss of 510 kW. Similarly, the estimated power consumption for the outer cavity would be approximately 950 kW. Total RF power consumption for a copper cavity, therefore, would be approximately 1.46 MW. We note that the cavity shape is not necessarily optimized for normal-conducting operation, and that several of the typical "tricks and techniques" (e.g. adding nosecones) may be able to significantly reduce this estimate; however, such work is beyond the scope of this initial study.

Assuming an average beam current of 1 A, and a beam kinetic energy of 1.45 MeV, the beam power would be approximately equal to the RF power required; a copper structure therefore may be feasible for meeting a ~50% wallplug efficiency target, given improvements to both the structure and RF source efficiency.

A normal-conducting design may also have a major advantage when it comes to radiation self-shielding. Since the inside surface of the cavity doesn't need to be kept at superconducting temperatures (which drives the cavity design towards thin niobium shells immersed in liquid helium), in principle the entire system could be made of two copper blocks, just as the 3D printed version was made. This would mean that there would be more mass between the treatment volume and the outside world. Alternatively, the space between the cavities could be backfilled with water or some other material which is a good, inexpensive shielding material.

Superconducting cavities

The ratio of the resistivities of room-temperature copper, to niobium at 4K and 350 MHz, is approximately 80,000:1. Operating at the same field gradients as above, with the same cavity profiles, a 4K Nb structure would require approximately 6.5 W for its inner cavity, and 12 W for its outer cavity. Assuming a 500:1 ratio for heat extraction [17] (e.g. one watt at 4K requires 500 W to remove to room temperature), a 10kW (wall-plug) helium refrigerator would be required to remove the waste heat from a superconducting radial RF gun operating at 4K. Note that these estimates are for removal of RF heat dissipation only; they do not cover static losses, radiative heat from cathode heaters, beam loss (e.g. halo), wakefields deposited by the beam, etc.

Cryo-cooled copper

Cryogenically cooled copper accelerating structures are an emerging technology. Cryogenically cooling copper to the range of 20 – 80 K provides benefits of significantly improved surface conductivity, while the required refrigeration system is simpler and more efficient than He refrigerators. While a detailed analysis of

‡ We proposed a LANL LDRD research project on this topic, which progressed to the final round of the selection process, but which was ultimately not chosen for funding.

this approach is beyond the scope of this document, recent results (albeit at high frequencies) [18] suggest that it bears consideration.

RF power couplers

We identified two potential methods for providing RF power to the RF structure.

An antenna (or e-probe) coupler can be inserted into an existing beamtube, or into a dedicated RF power port located at the cavity equator and azimuthally between two beamtubes. This concept was effectively demonstrated at 1/10-scale (geometric) via the cavity cold-test measurements. If required, the couplers could be DC-biased to suppress multipacting. This approach has the advantage of readily allowing variation in cavity coupling (for instance, to allow efficient operation at varying beam currents) via simple radial motion of the coupler. Its primary disadvantages are that a power coupler would displace a potential beamtube, and that using this method to provide power to inner cavities could prove problematic, especially if variable coupling is desired.

Alternately, a loop-type coupler could be located at the cross-sectional apex of the cavity, at the point of maximum magnetic field of the fundamental mode. This has the advantage of being very well-established in other cavities, such as storage-ring cavities, and can provide variable coupling via rotation of the loop. It is, however, arguably mechanically more complex than e-probe couplers, particularly if an SRF structure is used.

RF Power and Phase Stability

Our initial studies indicate that the relative phases between beam source, and the various cavity fields, must be maintained at ±1°, and the amplitude should be stabilized to < 1%. Given the state-of-the-art for currently operating accelerators, such as the Euro X-FEL [19], is approximately two orders of magnitude lower for both phase and amplitude jitter, this should be relatively easy to accomplish.

Beam Exit Window Options [20]

A critical issue is the design of the boundary that separates the high vacuum of the accelerator interior from the waste stream. There will be some energy loss in this window that will degrade the kinetic energy of the beam, and failure of this window due to excessive beam heating would be a catastrophic event, poisoning the cathode and contaminating the interior accelerator volume with waste stream material. For scanned linear beam systems this "window" is usually a strip of a thin metallic foil (typically a few mils of titanium) oriented lengthwise in the direction of the scan. For high-power operation the heat loading is reduced by the scanning action, and the window is convectively cooled by an air jet (a so-called air knife) along the length of the scan.

The beam kinetic energy loss can be estimated using

$$(dE/dx)/\rho = 2 \text{ MeV-cm}^2/\text{g} \qquad (2)$$

in which (dE/dx) is the electron stopping power in a material with density □. As an example, the kinetic energy loss in a one-mil titanium foil with density 4.2 g/cm^3 will be about 20 keV.

In the absence of cooling processes, the rate of temperature rise in the window, dT/dt, can be simply estimated according to

$$dT/dt = (Q/t)/(mc) = (dE/dx)\,(I/A) / (c\rho) \qquad (3)$$

in which Q is the electron beam energy deposited in the window in the time t, m is the mass of the window through which the beam passes, c is the specific heat of the window material, and (I/A) is the current density of the beam. For titanium, c = 0.5 J/g-^{o}C. A sure-safe design criterion used in the past is 0.1 mA/cm^2,

which gives a nominal temperature rise rate of 400 ^{o}C/s. The melting point of titanium is 1660 ^{o}C; thus, the window can be expected to lose strength if its temperature reaches ~800 ^{o}C. For the current density assumed above, this would occur in about two seconds. However, the convective cooling provided by an air knife can easily control this temperature rise.

From Table 1 the average beam currents of interest are of the order of one ampere. To meet the current density criterion cited above would require a window area of 10^4 cm^2. Assuming a beam height of 1 cm, the radius of the annular foil window would have to be ~16 meters, which is too large to be practical. For processing a flue gas stream, this issue does not appear to be too serious, however. Calculations indicate that the radius of the gas flow column will have to be fairly large in order to efficiently use the beam kinetic energy. In addition, stacking of multiple accelerator systems to decrease the current provided by a single system is a straightforward approach and would provide the important element of redundancy. For flue gas treatment it also may be possible to directly cool the thin exit window by diverting some of the waste stream itself, although this would require an interlock to terminate system operation if the flow of the waste stream were interrupted. What is clearly necessary is a realistic assessment of the sure-safe current density criterion, which is beyond the scope of this effort.

For waste water treatment the beam must penetrate the pipe that contains the flow, and this pipe must be of sufficient thickness and strength as to withstand the pressure of the stream. Again using titanium as an example, a wall thickness of 1/16th of an inch will result in a kinetic energy loss of 0.67 MeV, which is significant for the ~1 MeV beams under consideration. If the flow is confined to a simple pipe, the current loading of the pipe wall will be excessive. Assuming a 2-MeV beam with a current of 0.5 amperes, and a pipe radius of 1 cm, the current loading will be ~0.08 amps/cm^2. Even with the convective cooling provided by the waste stream, the resulting temperature rise rate is probably excessive. These considerations strongly suggest a large-radius, annular flow configuration for a liquid waste stream, with a beam kinetic energy as high as can be practically produced by the toroidal accelerator cavities.

Radiation Shielding and Beam Loss

One of the potentially promising features of the radial RF gun is its intrinsically "self-shielding" nature. The beam interaction volume can be designed so that the electron beam is fully absorbed within the media it is treating, as is the delivered radiation dose. Initial simulations have borne this out, indicating that in the energy range of Types I and II accelerators, with reasonable RF structure cavity wall thicknesses, a radial RF gun is intrinsically fairly well self-shielded along its equatorial plane. (The simulations shown in Figure 18 do not include any shielding above or below the structure.) An exception to this observation are sight lines along the beam flight tubes, as these provide an essentially unshielded pathway for forward-directed radiation from an opposing flight tube's beam.

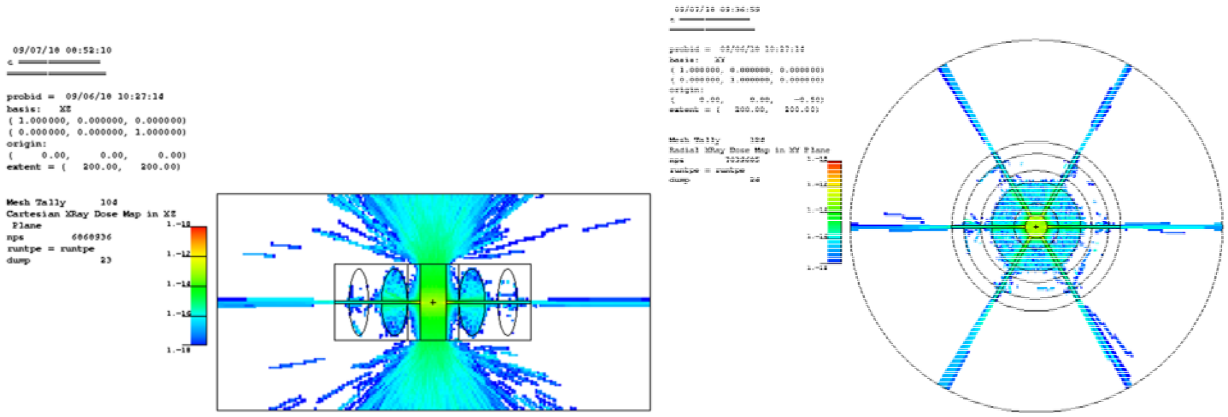

Figure 18: equatorial (left) and polar (right) view of X-ray dose maps.

This can be partly mitigated, however, by the use of an odd number of beam flight tubes, since then each flight tube is "facing" a blank wall (or diagnostics block, as above); then, most of the radiation propagating along a flight tube should be backscatter.

Shielding would still be desirable behind each beam flight path, and an overall enclosure for the structure, providing for RF and high-voltage protection as well as radiation shielding, is likely warranted.

Operational Estimates

Overall, we estimate that the radial RF gun could be available for 48 – 50 weeks out of a year, otherwise in 24/7/365 operation minus small interruptions for trips. The out-of-service time is expected to split approximately evenly between scheduled maintenance intervals, and unscheduled repair services due to significant faults or failures that are beyond the scope of the quasi-autonomous control system to address.

Scheduled Maintenance Intervals

Developing maintenance requirements based on the materials being treated is beyond the scope of this document. For the radial RF gun itself, however, either a one- or a two-week period, alternating annually, should suffice for routine maintenance: inspection and service of the vacuum system, inspection and service to the cryogenic refrigerator, RF system tests, e-gun test and cathode replacement if warranted by number of hours in service, etc. The longer down-times would be used for tasks that require the accelerator to be returned to room temperature, e.g. venting the cavity due to cathode replacement, or significant maintenance on the cryogenic systems.

Note that the expandability offered by the radial RF gun concept enables system designs which may have no *system* downtime. For example, if four guns were arrayed along a pipe through which the material to be treated is flowing, and each gun were capable of delivering a maximum dose equal to one-third of the required dose, having four guns would allow each gun to be operated at 75% during normal operation (likely contributing to longer mean time between failure for each gun). In the event of a fault in one of the guns, the other three could be increased to full power while the fault was corrected or the defective unit replaced. This could also apply for maintenance, allowing maintenance to be performed on one unit without requiring the overall system to be shut down. This would require the guns to be sufficiently separated, and for sufficient radiation protection to be installed, to enable safe access to one unit while the other units remained in operation.

Achievable Uptime

There are four major subsystems to be considered for the radial RF gun: the RF power system; the beam generation system; diagnostics, controls and power supplies; and the cryogenic refrigeration system. While these considerations are discussed in somewhat more detail below, our high-level expectation of achievable uptime is 97 – 98%, or approximately 7 – 11 days net down over a calendar year. This is based upon the overall uptime experience of users of high-power CW UHF klystrons, such as synchrotron X-ray sources, and the expectation of cryoplant availability for the LCLS-II project[§]. While a single radial RF gun installation is much smaller than either APS or LCLS-II, our presumption is that several systems would be installed at a given location; thus comparisons with facilities is arguably more apt than with standalone small-scale systems. We also note that other commercial / industrial accelerators of similar physical scale, e.g. X-ray radiotherapy systems for cancer treatment, have far lower average power output, as well as significantly different operating and likely regulatory environments, and are arguably not as good exemplars for comparison .

Under a "call-in" service model for system repairs, recovery time for serious faults could be extended by the time required for a service team to arrive on-site.

RF systems

Estimates of RF system-related downtime can be based on the experience of 3rd-generation X-ray synchrotron sources such as the 352-MHz klystrons at the Advanced Photon Source (APS) [21], which utilize CW MW-class klystrons similar to those that would be required to drive a radial RF gun. High-power CW klystrons, with output power from 0.5 – 1 MW and frequencies ranging from 325 – 1000 MHz are available

[§] The LCLS-II cryoplant is based in large part upon the upgraded cryoplant at Jefferson Lab.

from several commercial sources; solid-state sources may also become an increasingly viable option in the near future [16].

We use operational statistics from the APS to aid in our uptime estimates; these statistics are available online [22]. We will focus on the FY2017 statistics as it represents the latest full-year set of data.

Over the FY2017 run period, unavailability due to RF systems as a whole was 0.35% of scheduled hours, or 17.5 hours out of a scheduled 5000 hours. This figure "wraps up" both the storage ring RF systems, as well as any RF-related faults in the injector linac, and therefore provide somewhat of an overestimate. RF systems had a fault rate of 0.035 / day, or approximately 1 month mean time between faults. The mean fault recovery time would appear to be approximately 1.5 hours; however, it is more likely that faults represent a mix of mostly very fast recoveries (on the order of seconds to a few minutes, e.g. a simple trip reset), combined with relatively few numbers of more significant events requiring larger recovery and repair times.

Extrapolated to a 24/7/365 operating regime, and maintaining the same achievable uptime, a radial RF gun-based processing system could be expected to be unavailable for approximately 1.5 – 2 days per year due to RF system faults.

The APS incorporates a waveguide switching system for both its storage ring / booster 352-MHz RF systems [23], and its linac S-band RF systems. This allows a quasi-arbitrary mapping of klystron power source, to RF cavity to be driven, in turn facilitating (for instance) the rapid "swap-out" of a failed klystron without requiring an immediate physical replacement. (It is not a "power combiner" system.) Such a system could readily be incorporated into an industrial setting with N installed beam sources fed by a switching network of (N+M) RF sources. Such an approach would improve the probable uptime statistics, with a concurrent fractional increase in cost of (N+M)/N.

Cryogenics

The scale of refrigerator capacity required for a radial RF gun lies somewhere between that needed for commercial / medical devices such as MRI machines, and those required for superconducting accelerator facilities such as CEBAF, LCLS-II and RHIC; while the physical scale is much closer to the former, the operational requirements (e.g. dynamic heat loads from RF) are arguably closer to the latter. For a simple estimate, we extrapolate values for the LCLS-II cryoplant [24]: an expected availability of 98.6%, a nominal scheduled maintenance of 6 weeks in duration, and an estimated continuous operation of two to five years without a scheduled shutdown. For our estimation, we assume an annual shutdown of two weeks for maintenance, plus 98% availability during scheduled operating hours.

An alternate, for 4K operation, would be to outfit each radial RF gun with a series of smaller cryocoolers. These typically require service every 13,000 hours [25], or 1.5 years, so a preventive maintenance "swap-out" regime at yearly intervals would be reasonable.

Beam Generation

We assume the use of a COTS or near-COTS gridded cathode as the beam source, combined with modest high voltage (~25 kV) COTS power supplies. Apart from details of the physical electrode shapes (for initial beam focusing) the beam generation system represents highly mature, readily available technology. Uptime is expected to be greater than 99% following the initial "infant mortality" period common to most electronics, and no annual maintenance requirements. Based on experience with similar cathodes in related operating conditions and environments, such as microwave tubes, a 20,000-hour replacement time is a reasonable estimate. To first order, trips should be resettable almost immediately and the fault rate should be low compared to the other potential sources of faults.

The use of multiple cathodes can also increase system redundancy. Each cathode could be operated below its maximum rated current, so that if one cathode or electron gun were to fail, the rest of the cathodes could

simply be operated at higher current to ensure the same total current delivered to the treatment volume, although care would have to be taken to ensure that dose uniformity was preserved.

Controls and Power Supplies

For estimates of control and power supply uptimes, we again turn to the Advanced Photon Source for reference. For FY2017, Diagnostics had an uptime of 100%, power supplies of 99.61%

Other Sources of Downtime

The APS FY17 reliability summary includes a total of 1.6% downtime for "other" reasons, unattributable to or otherwise not clearly assignable to any other listed category on their reliability summary. This accounts for fully half APS's FY17 unscheduled downtime.

Staffing Requirements for Operations and Maintenance

As envisioned, a radial RF gun represents a high-power radiation generating device; although it will generally operate below the nominal neutron production threshold (7 – 10 MeV, depending on the target and the regulatory body), there are national- and state-level regulatory requirements regarding the required minimum staffing of its control area during operation. At a minimum, we would anticipate needing at least one staff member to be physically present in the control area during operations.

As far as active participation required by an operator to run the beam source, however, our expectation is that one operator should generally suffice for routine operations, as a given radial beam source should be almost fully automatable; the operator need not be an expert in accelerator operation per se. A modern control system should be able to perform automated startup and safe shutdowns of the various subsystems (RF, cryo, etc.) from and to a "cold" state. Simple feedback routines, combined with integrated diagnostics, should suffice to allow the radial RF gun to be brought to a given operational state: primarily, producing the desired beam energy and beam current, but perhaps also including which beam lines to energize should that be a design requirement. Machine protection features can incorporate a degree of autonomous decision-making, to enable the control system to determine whether a fault is "recoverable" or whether an expert must be called to assess and adjust the operation.

In most circumstances, we would anticipate the staffing requirements for maintenance would again be representable by a single trained but non-expert individual, with most routine maintenance involving the flow path of the material to be treated, rather than the accelerator itself. In the case of maintenance for the accelerator, we would recommend the use of external service companies to perform routine or preventive maintenance such as cathode changes, helium gas recharge for the cyro systems, etc. (This is the way many accelerator facilities in Japan tend to operate, for instance.) Similarly, most failure points we considered (e.g. vacuum system breach) would likely require expert outside intervention. Thus, we do not foresee an advantage to having an on-site maintenance staff for radial RF guns, given suitable per-unit reliability, unless the number of installed systems grows to the point where multiple serious faults per week are anticipated across the facility.

Cost Estimates

Capital Costs

A rough estimate of the RF power system can be made by using a "rule-of-thumb" of $5-$10/watt average power, installed, depending on the particulars of the source (e.g. frequency), RF system design specifics, quantity ordered etc.

Based on similar size accelerator structure fabrication, we estimate the cost of a radial RF gun at between $2M-$5M.

Assuming static and other "parasitic" heat loads (e.g. beam loss) are low enough, a number of small cryocoolers could be used instead of a monolithic cryoplant. The cost estimate is approximately $23k/watt removed at 4K; so the cryogenic system is estimated to cost approximately $400k, assuming 18.5 W dynamic loss, 10 W static loss, and 5 W parasitic / overhead. For larger installations the cost of a monolithic cryogenic plant with distribution system would need to be compared to the cost of outfitting each radial RF gun with its own independent cryocooler system.

We estimate the remaining cost of hardware (cathodes, power supplies, etc.) at $100k.

Thus, we estimate the installed cost of a single radial RF gun at between $7.5M - $15.5M, depending on the system particulars (frequency, number of beam tubes, static and dynamics RF loads, etc.). We anticipate the per-unit cost could be reduced, perhaps significantly, if installed in large numbers.

Operating Costs

Manpower (Operations Staff)

Given a sufficiently autonomous control system, a single staff member should be capable of monitoring and providing overall control for a number of Type I or Type II-class beam sources. Given 24/7/365 operation, that suggests on the order of 5 full-time employees (FTE) per year would be the minimum manpower requirement: 1 person / shift, 3 shifts / day, and allowing for time-off, sick leave and holiday coverage.

Service and Repair

As above, we anticipate either a one- or a two-week maintenance period, alternating annually. As a strawman service plan, we would anticipate two-person teams specialized by area: RF, cryogenics, and controls / power supplies / vacuum. For annual service periods, a team for each area would be expected to be on-site and performing work; for repair calls, only the specific team to address the trouble area would likely need to be called in. Broadly, however, such a level of effort represents on the order of two FTE-months.

Electrical

The average cost for industrial electrical power varies considerably by state [26], but for comparison purposes we will use a nominal $0.10/kilowatt-hour.

Based on the total power consumption estimate from Table 3, estimated per-hour electrical costs are $174/hour, or $1.52M/year for 24/7/365 operation per unit generating 1 MW of beam power. Note that we are excluding the cost of cooling the RF system, as this depends very heavily upon both the RF system efficiency, and other resources available to aid in waste heat removal. For instance, if treating a wastewater stream, it is feasible to consider using the flow itself as a heat sink.

Table 3: System-level power consumption estimates

System	Consumption (kW)	Notes
RF power	1700.0	1 MW to beam, 60% efficiency
RF system cooling		(tbd)
cathode heaters	0.1	
e-gun HV system	28.0	25 kV x 1 A to beam, 90% efficiency
cryo system	10.0	assuming 4K operation
controls / diagnostics	2.0	
vacuum pumps	2.0	
Net power consumption during operation	42.1	

References

1 https://science.energy.gov/hep/research/accelerator-stewardship/
2 DOE National Laboratory Announcement Number LAB 17-1779.
3 J.W. Lewellen and J.R. Harris, "Radial Radio Frequency (RF) Electron Guns," U.S. Provisional Patent Application 62/577,561, 26 OCT 2017.
4 J.W. Lewellen, F.L. Krawczyk and J.R. Harris, "Design of a Radial RF Electron Gun," presented at the 2016 International Particle Accelerator Conference, March-April 2018, Vancouver, BC, Canada.
5 Y. Jongen *et al.*, "The Rhodotron, a new 10 MeV, 100 kW, cw metric wave electron accelerator," Nucl. Instrum. Meth **B**79 (1993), pp. 865-870.
6 https://www.cst.com
7 Poisson Superfish, http://laacg.lanl.gov
8 https://www.cathode.com
9 Pulsar Physics, http://www.pulsar.nl
10 Emilio A Nanni et al, "Prototyping high-gradient mm-wave accelerating structures," 2017 *J. Phys.: Conf. Ser.* **874** 012039
11 https://www.pasternack.com/images/ProductPDF/RG402-U.pdf
12 P. McChesney, "Multi-plate Interceptive Electron Beam Energy Diagnostic -- Theoretical Design," submitted to AIP Advances (2018).
13 P. McChesney, J. Cardenas, J. Love, J.R. Harris, R. Cooksey, J.W. Lewellen, B. Berls, C. O'Neill, K. Folkman, and J. Stoner, "Multi-Plate Interceptive Electron Beam Energy Diagnostic -- Implementation and Validation," submitted to AIP Advances (2018).
14 P. McChesney, J. Cardenas, J. Love, J.R. Harris, R. Cooksey, J.W. Lewellen, B. Berls, C. O'Neill, K. Folkman, and J. Stoner, "A High Dynamic Range Interceptive Electron Beam Charge Monitor," submitted to Physical Review Accelerators and Beams (2018).
15 Private communication, M. Kirshner (AOT/LANL), September 2018.
16 Private communication, D. Horan (APS/Argonne), May 2018.
17 Private communication, T. Smith (Stanford University), 2008.
18 Reference to cryo-cooled copper structure development.
19 *The Technical Design Report (TDR) of the European XFEL*, available online at http://xfel.desy.de/technical_information/tdr/tdr/
20 This section taken from R.B. Miller and N.T. Myers, "Preliminary Systems Analysis of a Novel Waste Treatment Concept," Leidos/AFRL internal working document, 28 SEPT 2018.
21 D. Horan, G. Pile and A. Cours, "352-MHz klystron performance at the Avanced Photon Source," Presented at the 1999 Particle Accelerator Conference, https://accelconf.web.cern.ch/accelconf/p99/PAPERS/MOP153.PDF
22 https://ops.aps.anl.gov/statistics/
23 Y.W Kang and D. Horan, "Reconfigurable high-power RF system in the APS," https://inis.iaea.org/collection/NCLCollectionStore/_Public/29/024/29024209.pdf
24 LCLS-II final design report, available online at https://portal.slac.stanford.edu/sites/ard_public/people/tora/Temp/150921%20LCLS-II%20FDR.pdf, Chapter 7.
25 Private communication, Dan Logan, Janis, January 2018.
26 https://www.rockymountainpower.net/about/rar/ipc.html